A Markerless Joint Detection through a Hand Geometric Representation

Aline de Faria Lemos[a] and Nagy Balázs Vince[b]
Department of Mechatronics, Optics and Mechanical Engineering Informatics,
Budapest University of Technology and Economics, Műegyetem rakpart 3. Bldg D, Budapest, Hungary

Keywords: Joint Position Estimation, Human Hand, Particle Swarm Optimization, Genetic Algorithm, Image Processing, Optimization.

Abstract: In several fields, such as man-machine interface and occupational therapy, the human hand-joint position is required. Traditional methods usually rely on image processing allied with marker placement, e.g. reflexive marker, which can be time-consuming and uncomfortable for the subject. For these reasons, scientific efforts are being made to create reliable and convenient joint tracking. This paper proposes a methodology that generates geometric figures to mimic the hand configuration. This process is made possible by an optimization algorithm, which finds the most suitable placement of these geometric shapes. One time the real hand and the created representation share similar features, the joints position can be estimated. Two optimization algorithms were employed: particle swarm optimization and genetic algorithm. In both cases, satisfactory results were obtained. Although, particle swarm optimization marginally outperformed the latter method.

1 INTRODUCTION

The human hand and its ability to manipulate objects with dexterity are hallmarks of human evolution. It is through the hand that much of the mechanical human iterations with the world take place. The hand performs mechanical tasks ranging from the use of high force to functions that require delicacy and precision (Leon et al., 2013; Barroso, 2010). The versatility of the hand is possible due to the complexity of its structure and its refined control, which enable the execution of multi-digital prehension and pinch movements (Hagert et al., 2012; Souza et al., 2015). The study of the human hand and the characterization of pinch function have an important role in multiple fields (Grujić and Bonković, 2015), such as the study of pathologies (Kingsbury et al., 2014; Barroso et al., 2011; Coimbra, 2011), rehabilitation of upper limbs (Musiolik, 2008; Barroso et al., 2011; Neves, 2011), development of man-machine interface (Matsubara and Morimoto, 2013; Adams et al., 2015; Endo and Kawasaki, 2015), design of robotic arms and biomechanical models (Leon et al., 2013; Saikia, 2014; Quigley et al., 2014; Deimel and Brock, 2016).

The analysis of hand articular movement can be performed by different equipment or procedures. Traditional methods usually rely on manual measurements, e.g. manual goniometry, or marker-based techniques, e.g. stereophotogrammetry (Barroso et al., 2007). Although the manual goniometer is the most frequently used technique, its inter-rater reliability is criticized (Crasto et al., 2015). On the other hand, marker-based techniques can be time-consuming and uncomfortable for the subject. Nowadays, the literature contains promising markless solutions for hand tracking and pose estimation (Zhou et al., 2016; Supancic et al., 2015; Sridhar et al., 2015; Mueller et al., 2017; Mueller et al., 2018). However, no benchmark was established. For this reason, hand joint estimation is still an open research challenge. This work presents a methodology to generate a geometric human hand model. The underlying concept of generation process leverages image processing allied to optimization methods. From this model, joint positions are estimated, which composes in the main goal of the paper: a markerless hand joint detection method.

2 METHODOLOGY

The present study consists of a human hand joints detection algorithm, which is composed of digital image processing allied to optimization techniques. The method is based on reconstructing the pose present

[a] https://orcid.org/0000-0001-9898-6370
[b] https://orcid.org/0000-0002-8489-7200

Lemos, A. and Vince, N.
A Markerless Joint Detection through a Hand Geometric Representation.
DOI: 10.5220/0008971706260633
In *Proceedings of the 12th International Conference on Agents and Artificial Intelligence (ICAART 2020) - Volume 2*, pages 626-633
ISBN: 978-989-758-395-7; ISSN: 2184-433X

in certain hand image by placing polygons over the hand dorsal surface and hand segments, creating a low-resolution representation of the hand based on geometric shapes where all the geometric properties are known. For instance, hand segments can be approximated by rectangles, information about the actual shape of the segment is lost. However, information about the position and dimension is preserved.

Conceptually, it is easy to grasp the feasibility of the task in hand. The human mind can trivially draw a geometric representation of the hand which captures relevant information about joints' position, Fig.1 shows such representation. The procedure to automatically create this representation can be interpreted as a search algorithm, where the parameter space is composed of shape's definitions. Particle Swarm Optimization (PSO) and Genetic Algorithm (GA) were proposed to find the most suitable configuration according to the divergence from the hand and the geometric representation. The remainder of the section explains in detail each step of the procedure.

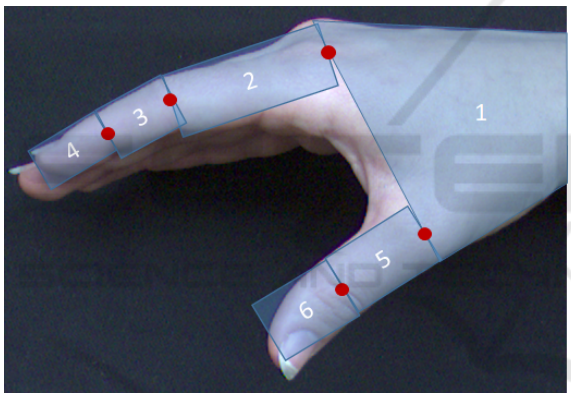

Figure 1: Illustration of a possible arrangement of the drawn polygons, in contrast to a hand picture.

2.1 Cost Function

The cost function is summarized in the Fig. 2. It receives a series of geometric figures parameters as input and is composed of two modules, "Draw polygons" and "Pattern recognition". The first creates an illustration of the human hand by using geometric figures, which are drawn by using the parameters contained in the particle values. The second uses a pattern recognition technique, based on XOR logical operation, to compare the polygons image to a picture of the human hand. The function outputs the area percentage of the resulting image in relation to the hand picture. The mentioned modules are detailed in the following subsections.

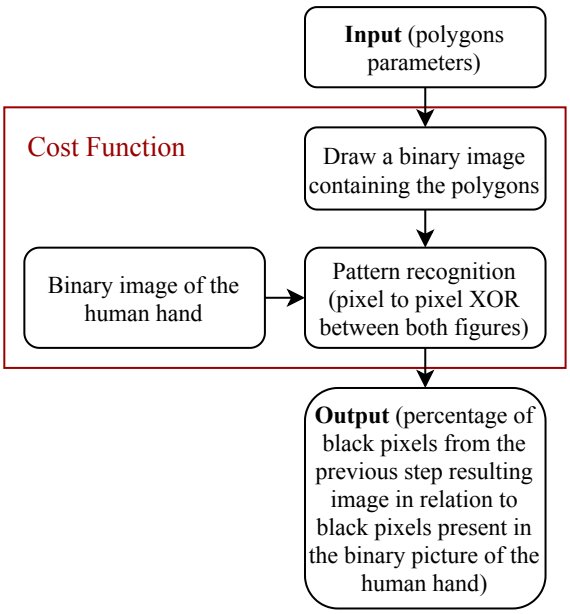

Figure 2: Cost function block diagram.

2.1.1 Draw Polygons Module

"Draw polygon" is the module responsible for creating a new binary image containing six geometric figures: one trapezium and five rectangles. These polygons are meant to compose an illustration that imitates the posture of a human hand in a superior view. Fig. 1 illustrates a possible arrangement of the geometric figures in contrast to a hand picture. The polygons are mandatorily connected to each other by their extremities. The advantage of this constraint is twofold, it ensures physiology soundness (since it is known the linkage between segments), and reduces the complexity of the task (since it lowers the number of parameters to be defined). These connections are also the estimated joint positions and are illustrated by the red dots present in Fig. 1. For the purpose of facilitating joint referencing, they were enumerated in the following sequence: index finger metacarpophalangeal, proximal and distal interphalangeal joints and thumb metacarpophalangeal and interphalangeal joints, as illustrated in Fig. 3a

The polygons are drawn considering that the hand is executing a cylindrical pinch movement. In this case, the first polygon to be drawn is a trapezium, which represents the dorsal surface of the hand. Rectangles 2, 3 and 4 correspond to proximal, medial and distal phalanges of the index finger. Similarly, rectangles 5 and 6 stand for proximal and distal phalanges of the thumb.

The geometric figures are created from their vertex points, which are calculated from the parameters

shown in Fig. 3b. They are the input of the cost function and, consequently, the particle value, which includes 23 variables. In this figure, D indicates a dimension, θ are the rectangles angular positions and P is a Cartesian point. The particle includes only the y coordinate of the points $PR2$, $PR5$, $P1$ and $P2$ and both y and x coordinates of the points $P3$ and $P4$. The first number of this nomenclature correlates to the polygon index. On the other hand, the second number classifies the variable into height (1) or width (2). Table 1 contains all cost function input variables, along with their description.

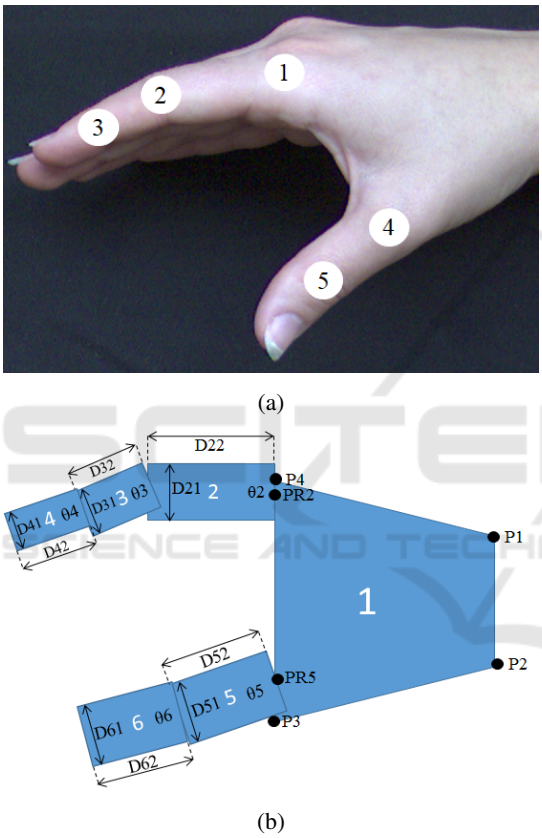

Figure 3: Illustrations containing the adopted nomenclature. a) Joint enumeration for the purpose of facilitating joint referencing. b) Cost function input data used to create the polygons.

2.1.2 Pattern Recognition Module

The polygons image, generated on the ”draw polygons” module, is compared to a human hand picture to achieve the polygons' best positions and dimensions. To proceed with this comparison is crucial to segment the hand picture by extracting the hand region from the image background. Thresholding was the elected segmentation approach for this purpose. In this method, the hand image, acquired in RGB, is converted to grayscale. Then, the foreground is extracted from the image by applying thresholding to the grayscale image, which results in a binary image of the hand.

Table 1: Description of the cost function input data used to create the polygons.

Variable	Related Polygon	Description
$P1_y$	1	y coordinate of vertex 1
$P2_y$		y coordinate of vertex 2
$P3_x$		x coordinate of vertex 3
$P3_y$		y coordinate of vertex 3
$P4_x$		x coordinate of vertex 4
$P4_y$		y coordinate of vertex 4
$D21$	2	Polygon height
$D22$		Polygon width
$PR2_y$		y coordinate of $PR2$ point
θ_2		Polygon angular position
$D31$	3	Polygon height
$D32$		Polygon width
θ_3		Polygon angular position
$D41$	4	Polygon height
$D42$		Polygon width
θ_4		Polygon angular position
$D51$	5	Polygon height
$D52$		Polygon width
$PR5_y$		y coordinate of $PR5$ point
θ_5		Polygon angular position
$D61$	6	Polygon height
$D62$		Polygon width
θ_6		Polygon inclination angle

A pixel to pixel XOR logical operator is applied to perform the comparison between the polygons image and the binary human hand image. It consists of an XOR operation between each pixel of the polygons image and its correspondent pixel in the hand image, similarly to methods present in the available literature (Bovik and Desai, 2000; Koukounis et al., 2011; Mookdarsanit et al., 2015; de Faria Lemos et al., 2017). An analogous procedure is illustrated in Fig. 4. In this figure, $I1$ represents a setpoint image to which image $I2$ will be compared. The pixel to pixel XOR operation is applied to these images (second line of the illustration), resulting in the last figure of the illustration.

The output of the ”pattern recognition” module is the percentage between the number of black pixels in the resulting image of the XOR operation and the number of black pixels in the binary hand picture.

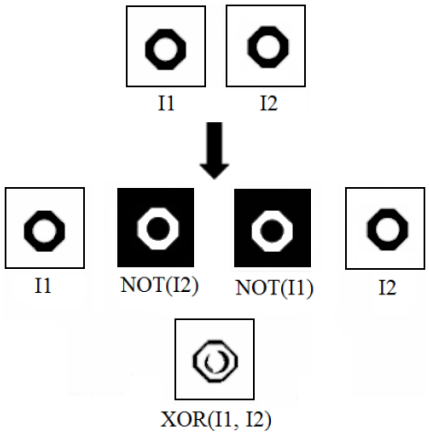

Figure 4: Illustration of a pattern recognition procedure by using a pixel to pixel XOR operation. Source: (Bovik and Desai, 2000), modified.

2.2 Optimization

Evolutionary algorithm is a set of algorithms applied in complex search and optimization tasks, which resemble natural evolution. Based on Darwinian evolutionary theory, genetic algorithms are the most popular techniques among them (Mirjalili and Lewis, 2016; Rashedi et al., 2009). In these algorithms, a population of candidate solutions is, usually, randomly generated and evaluated to select population members who survive to reproduce. A recombination process builds new individuals by application of the crossing operator on the selected individuals and mutation is applied to the descendants (Holland, 1992; Holland et al., 1992; Sastry et al., 2005).

Proposed by Eberhart and Kennedy (Eberhart and Kennedy, 1995), particle swarm is an optimization algorithm based on social–psychological principles. In this algorithm, all particles survive, contrary to the selection method, used in evolutionary algorithms (Kennedy, 2010). The method simulates birds' predatory behavior and uses the input parameters to define a particle in the high dimension search space. The searching direction of each particle is updated by its best solution and also by a global best solution, which is the best solution among all the particles that compose the swarm (Rashedi et al., 2009; Feng et al., 2018).

To optimize the cost function, described in the previous subsection, the MatLab modules "ga" and "particleswarm" were elected to perform genetic algorithm and particle swarm optimization, respectively. The first used gaussian mutation with a migration fraction of 0.2. Similarly, crossover rate, pareto fraction and population size were selected as 0.8, 0.35 and 200. As for the latter, the optimization parameters chosen for PSO were adaptive inertia with a range of 0.1 to 1.1, swarm size, learning factor of cognitive component and social component were respectively set to 100, 1.49 and 1.49. The parameter sets for both optimization methods were chosen by an iterative approach, in which the best parameter combinations were selected from the several tested groups.

Both methods shared the same input images and search spaces for comparison purposes. However, five different scenarios were created to provide sensitivity analysis. The range of rectangles angular positions were fixed as 45 degrees in all simulated scenarios. In contrast, the range of point positions and dimensions started with the amount of 10 pixels and increased to 20, 30, 40 and 50 pixels on subsequent scenarios. These range values were chosen to vary around the smallest hand segment dimension, which corresponds to the width of the index finger distal phalanx, approximately 40 pixels.

2.3 Images Acquisition

The human hand pictures used as comparison images of the pattern recognition module are presented in Fig. 5. These images were captured from a single subject while performing cylindrical pinch movements in a controlled environment. They were acquired by a Basler $acA640-750um$ USB 3.0 camera with resolution (HxV), pixel size (HxV) and frame rate of 640 px x 480 px, 4.8 μm x 4.8 μm and 751 fps equipped with Basler lens $C23-1216-2M$ with fixed focal length of 12 mm, aperture range from $F1.6$ - $F16$ and a resolution of 2 megapixels.

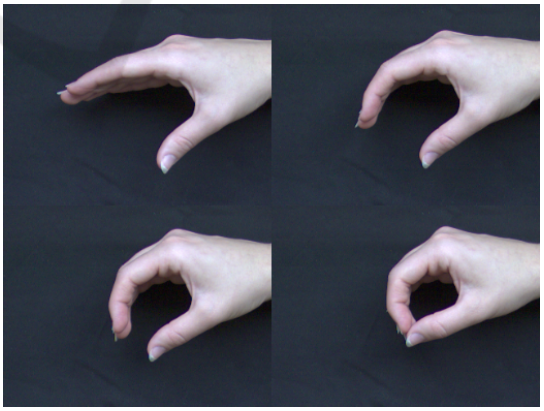

Figure 5: Pose images used in the experiment. These images were acquired from a single subject while performing a cylindrical pinch movement.

3 RESULTS AND DISCUSSION

This work aims to estimate five human hand joint positions, which are enumerated in Fig. 3a, from hand images. These images were acquired from a single subject while performing a cylindrical pinch movement. In total, 4 different pose images were used in the experiment, as presented in Fig. 5. For each pose, 5 distinct ranges of search space were selected, as discussed in section 2.2, and all tests were performed using both optimization methods: PSO and GA. In summary, 40 particular experiments were performed, totalizing in 200 estimated joint positions.

In order to quantify the estimated joint positions' performance, the positions of the joints were compared with the human-annotated position. Naturally, the actual location of the joint is not a single point, rather a region. These regions were defined as circumferences of 20 pixels radius for joints 1, 4 and 5 and 15 pixels radius for joints 2 and 3. The center of each region was chosen as a physiologically suitable point for the joint position. The interpretation of the positive result is here defined as a point that falls inside these regions, Table 2 synthesizes the results achieved according to each scenario. Table 2 also shows the maximum, minimum and average performance of the scenarios in terms of the cost function values described in section 2.1.2.

Considering all 20 experiments performed by each optimization method, PSO outperforms GA in the overall accuracy of positive results, with an assertive rate of 82% of estimated joints placed inside the fitting regions, in contrast to 80% correctly estimated by GA. PSO also achieved greater performance, with 8.8% on average in terms of the cost function values, while GA obtained 10.1%.

The performance of the methods can also be estimated by the distance between the output and the center of the fitting regions. These differences are labeled from this point of the text as position errors. Fig. 6 shows the behavior of the distance from the center of the joint over the adopted ranges. Even though a clear relationship between the performance and adopted range does not arise in either method, PSO showed less variance in performance. It is worth to mention, that the adoption of greater pixel range translates to a more generalist method, allowing a wider gamma of hand sizes.

The performance of the method can also be visualized grouped by joint individually, as shown in Fig. 7. This figure displays the dispersion of the position errors for each optimization method in contrast to the fitting regions. At first glance, it can be noticed that for the majority of the joints present a component

Table 2: Results achieved by both optimization methods according to each range of search space. Maximum, minimum and mean percentage refers to the performance of the scenarios in terms of the cost function values and positive results indicate the total of assertive estimated joints.

Adopted Range	Comparison Parameter	PSO	GA
50 px	Max. pct. [%]	7.1	9.3
	Min. pct. [%]	6.3	7.4
	Mean pct. [%]	6.9	8.1
	Positive results	15/20	17/20
40 px	Max. pct. [%]	8.0	12.7
	Min. pct. [%]	5.8	8.7
	Mean pct. [%]	7.0	10.2
	Positive results	19/20	14/20
30 px	Max. pct. [%]	10.7	10.6
	Min. pct. [%	7.0	8.1
	Mean pct. [%]	8.8	9.5
	Positive results	15/20	18/20
20 px	Max. pct. [%]	9.9	10.6
	Min. pct. [%]	8.0	8.7
	Mean pct. [%]	8.9	9.6
	Positive results	17/20	15/20
10 px	Max. pct. [%]	17.4	17.5
	Min. pct. [%]	8.8	9.0
	Mean pct. [%]	12.4	12.9
	Positive results	16/20	16/20

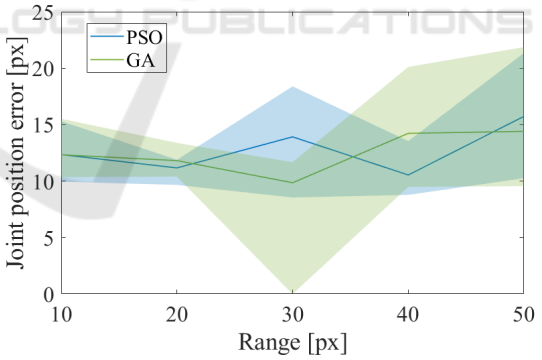

Figure 6: Sensibility analysis: Distance from region center versus range.

of systematic error. However, the number of experiments executed at this point is not large enough for drawing conclusions. Future possibilities regarding this fact will be mention on 4. On the other hand, it is clear that there is a predominance of position errors within the fitting position.

Fig. 8 exemplifies the joint tracking result for an arbitrary position and range. The figure is referent to the result of the Particle Swarm Optimization method. Because of the consistency across simulations led the

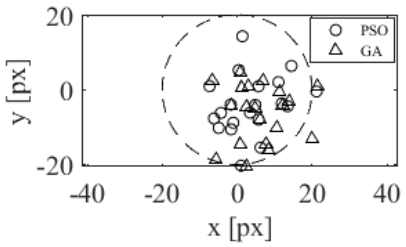

(a)

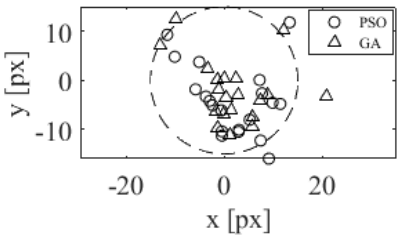

(b)

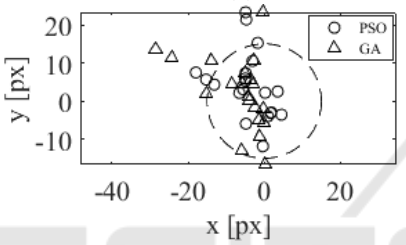

(c)

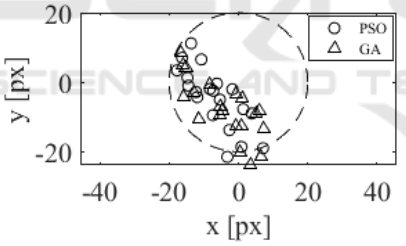

(d)

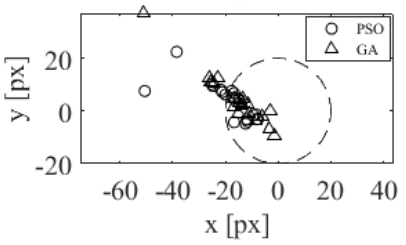

(e)

Figure 7: Dispersion of the position errors for each optimization method in contrast to the fitting regions (dashed line). a) Joint 1 - metacarpophalangeal joint of index finger; b) Joint 2 - proximal interphalangeal joint of index finger; c) Joint 3 - distal interphalangeal joint of index finger; d) Joint 4 - metacarpophalangeal joint of thumb; e) Joint 5 - interphalangeal joint of the thumb.

authors to elect it as the standard method of optimization. In the first image, Fig.8a, it is shown the output of the XOR operation between the binary image of the hand and its geometric representation. While in Fig.8b the overlapped image from the hand and the estimated joints are exhibit.

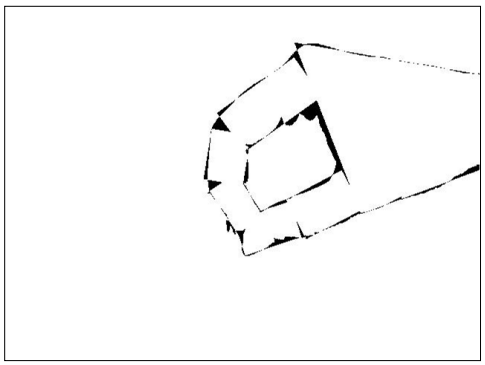

(a)

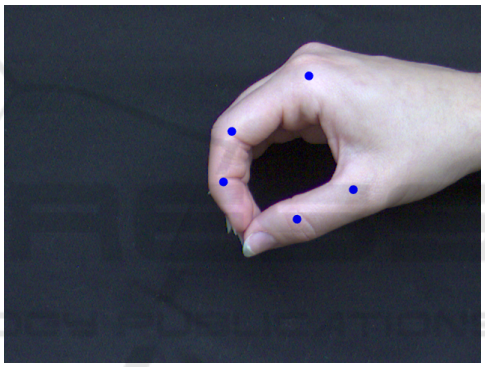

(b)

Figure 8: Example of a joint tracking result for an arbitrary position and range. a) Output of the XOR operation between the binary image of the hand and its geometric representation. b) Overlapped image from the hand and the estimated joints.

4 CONCLUSIONS AND FUTURE WORK

The position tracking of the hand joints has a diverse gamma of application. Even though the literature offers some solution, there is no convergence or established approach. This work presented a novel algorithm which utilizes two metaheuristic search approach allied to a simple image processing technique to build a geometric representation of the human hand while performing cylindrical pinch. From this model is possible to derive joint positions through markerless digital images, information which is crucial in certain fields, such as occupational therapy.

Future works should be carried out addressing but not limited to these shortcomings:

1. **Data Collection:** As pointed out previously, the lack of standardized, open-sourced dataset still limits research in the field. Data collection should be carried out to support more robust solutions.
2. **Models Building:** The search for the most suitable optimization method is far from exhausted, different solutions should be tested (e.g. artificial immune system).
3. **Models Integration:** Support models can be applied to boost effectiveness (e.g. population creation schemes, dynamic bounds, occlusion solver).
4. **Error Analysis:** Patterns in the error distribution might arise when considering a bigger dataset, which can be leverage (e.g. Error regression models).

REFERENCES

Adams, R., Olowin, A., and Hannaford, B. (2015). Gloved human-machine interface. US Patent 9,104,271.

Barroso, P., Vecchio, S., Xavier, Y., Sesselmann, M., Araújo, P., and Pinotti, M. (2011). Improvement of hand function in children with cerebral palsy via an orthosis that provides wrist extension and thumb abduction. *Clinical Biomechanics*, 26(9):937–943.

Barroso, P. N. (2010). *Nova Órtese de Extensão de Punho e Abdutora de Polegar para Crianças com Paralisia Cerebral: Avaliação de suas Contribuições para o Incremento da Funcionalidade Manual*. PhD thesis, Federal University of Minas Gerais.

Barroso, P. N., Nagem, D. A. P., Miranda, R. J. C., Kirkwood, R., and Pinotti, M. (2007). Quantitative analysis of thumb range of motion during functional activities. *19th International Congress of Mechanical Engineering*, 1:1–6.

Bovik, A. and Desai, M. (2000). *Handbook of Image and Video Processing*, chapter 2, Basic image processing techniques, pages 21–27. Academic Press, San Diedo.

Coimbra, D. F. M. (2011). O tratamento da rizartrose: Estado da arte. *Instituto de Ciências Biomédicas Abel Salazar*.

Crasto, J. A., Sayari, A. J., Gray, R. R., and Askari, M. (2015). Comparative analysis of photograph-based clinical goniometry to standard techniques. *Hand*, 10(2):248–253.

de Faria Lemos, A., da Silva, L. A. R., Furtado, E. C., and de Paula, H. (2017). Positioning error estimation of steel strips in steckel rolling process using digital image processing. In *2017 IEEE Industry Applications Society Annual Meeting*, pages 1–8. IEEE.

Deimel, R. and Brock, O. (2016). A novel type of compliant and underactuated robotic hand for dexterous grasping. *The International Journal of Robotics Research*, 35(1-3):161–185.

Eberhart, R. and Kennedy, J. (1995). Particle swarm optimization. In *Proceedings of the IEEE international conference on neural networks*, volume 4, pages 1942–1948. Citeseer.

Endo, T. and Kawasaki, H. (2015). A fine motor skill training system using multi-fingered haptic interface robot. *International Journal of Human-Computer Studies*, 84:41–50.

Feng, X., Ling, X., Zheng, H., Chen, Z., and Xu, Y. (2018). Adaptive multi-kernel svm with spatial-temporal correlation for short-term traffic flow prediction. *IEEE Transactions on Intelligent Transportation Systems*, 20(99):1–13.

Grujić, T. and Bonković, M. (2015). Measurement and analysis of human hand kinematics. *World Academy of Science, Engineering and Technology International Journal of Biomedical and Biological Engineering*, 9(2):97.

Hagert, E., Lee, J., and Ladd, A. L. (2012). Innervation patterns of thumb trapeziometacarpal joint ligaments. *The Journal of hand surgery*, 37(4):706–714.

Holland, J. H. (1992). Genetic algorithms. *Scientific american*, 267(1):66–73.

Holland, J. H. et al. (1992). *Adaptation in natural and artificial systems: an introductory analysis with applications to biology, control, and artificial intelligence*. MIT press.

Kennedy, J. (2010). Particle swarm optimization. *Encyclopedia of machine learning*, pages 760–766.

Kingsbury, S. R., Gross, H. J., Isherwood, G., and Conaghan, P. G. (2014). Osteoarthritis in europe: impact on health status, work productivity and use of pharmacotherapies in five european countries. *Rheumatology*, 53(5):937–947.

Koukounis, D., Nicholson, L., Bull, D. R., and Achim, A. (2011). Retinal image registration based on multiscale products and optic disc detection. In *2011 Annual International Conference of the IEEE Engineering in Medicine and Biology Society*, pages 6242–6245. IEEE.

Leon, B., Morales, A., and Sancho-Bru, J. (2013). *From Robot to Human Grasping Simulation*, chapter 5, The Model of the Human Hand, pages 123–174. Springer.

Matsubara, T. and Morimoto, J. (2013). Bilinear modeling of emg signals to extract user-independent features for multiuser myoelectric interface. *IEEE Transactions on Biomedical Engineering*, 60(8):2205–2213.

Mirjalili, S. and Lewis, A. (2016). The whale optimization algorithm. *Advances in engineering software*, 95:51–67.

Mookdarsanit, P., Soimart, L., Ketcham, M., and Hnoohom, N. (2015). Detecting image forgery using xor and determinant of pixels for image forensics. In *2015 11th International Conference on Signal-Image Technology & Internet-Based Systems (SITIS)*, pages 613–616. IEEE.

Mueller, F., Bernard, F., Sotnychenko, O., Mehta, D., Sridhar, S., Casas, D., and Theobalt, C. (2018). Ganerated hands for real-time 3d hand tracking from monocular rgb. In *Proceedings of the IEEE Conference on Computer Vision and Pattern Recognition*, pages 49–59.

Mueller, F., Mehta, D., Sotnychenko, O., Sridhar, S., Casas, D., and Theobalt, C. (2017). Real-time hand tracking under occlusion from an egocentric rgb-d sensor. In *Proceedings of the IEEE International Conference on Computer Vision*, pages 1284–1293.

Musiolik, A. (2008). Multibody model of the human hand for the dynamic analysis of a hand rehabilitation device. *Universidade Tecnica de Lisboa*.

Neves, D. R. (2011). Desenvolvimento de modelos biomecânicos tridimensionais do membro superior: mão e cotovelo. Master's thesis, Federal University of Minas Gerais, Minas Gerais, Brazil.

Quigley, M., Salisbury, C., Ng, A. Y., and Salisbury, J. K. (2014). Mechatronic design of an integrated robotic hand. *The International Journal of Robotics Research*, 33(5):706–720.

Rashedi, E., Nezamabadi-Pour, H., and Saryazdi, S. (2009). Gsa: a gravitational search algorithm. *Information sciences*, 179(13):2232–2248.

Saikia, G. (2014). Extending modules for icub simulator to emulate human grasp forms. In *Signal Processing and Integrated Networks (SPIN), 2014 International Conference on*, pages 636–640. IEEE.

Sastry, K., Goldberg, D., and Kendall, G. (2005). Genetic algorithms. In *Search methodologies*, pages 97–125. Springer.

Souza, L. K., Rezende, A. P., and Petten, A. M. V. N. (2015). O efeito da Órtese curta para rizartrose na força de preensão e força de pinça: Estudo de caso Único. *Revista de Terapia Ocupacional da Universidade de São Paulo*, 26:250–257.

Sridhar, S., Mueller, F., Oulasvirta, A., and Theobalt, C. (2015). Fast and robust hand tracking using detection-guided optimization. In *Proceedings of the IEEE Conference on Computer Vision and Pattern Recognition*, pages 3213–3221.

Supancic, J. S., Rogez, G., Yang, Y., Shotton, J., and Ramanan, D. (2015). Depth-based hand pose estimation: data, methods, and challenges. In *Proceedings of the IEEE international conference on computer vision*, pages 1868–1876.

Zhou, Y., Jiang, G., and Lin, Y. (2016). A novel finger and hand pose estimation technique for real-time hand gesture recognition. *Pattern Recognition*, 49:102–114.